

---

1  
2 This manuscript is a preprint and has been submitted to EarthArXiv. It is under peer review at  
3 *Nature Communications*. Please feel free to contact any of the authors directly to comment on  
4 the manuscript.  
5

---

6  
7 15<sup>th</sup> May 2023

8  
9 **Quantitative constraints on flood variability in the rock record.**

10 Jonah S. McLeod<sup>1\*</sup>, James Wood<sup>1</sup>, Sinéad J. Lyster<sup>1,2</sup>, Jeffery M. Valenza<sup>3</sup>, Alan R.T.  
11 Spencer<sup>1,4</sup>, Alexander C. Whittaker<sup>1</sup>.

12 <sup>1</sup>Department of Earth Science and Engineering, Imperial College London, UK, SW7 2BX.

13 <sup>2</sup>Department of Geosciences, The Pennsylvania State University, State College, Pennsylvania  
14 16801, USA.

15 <sup>3</sup>Department of Geography, University of California, Santa Barbara, 1832 Ellison Hall, Santa  
16 Barbara, California 93106, USA.

17 <sup>4</sup>Science Group, The Natural History Museum, London, UK, SW7 5HD.

18 \*jonah.mcleod18@imperial.ac.uk

19  
20  
21 ORCID: JSM – 0000-0002-5382-3559, JW – 0000-0002-1673-0097, SJL - 0000-0002-1188-  
22 533X, JMV - 0000-0002-1066-0817, ARTS - 0000-0001-6590-405X, ACW - 0000-0002-  
23 8781-7771  
24  
25

26 **ABSTRACT**

27 Floods determine river behaviour in time and space. Yet quantitative measures of discharge  
28 variability from geological stratigraphy are sparse, even though they are critical to understand  
29 landscape sensitivity to past and future environmental change. Here we show how storm-  
30 driven river floods in the geologic past can be quantified, using Carboniferous stratigraphy as

31 an exemplar. The geometries of dune cross-sets demonstrate that discharge-driven  
32 disequilibrium dynamics dominated fluvial deposition in the Pennant Formation of South  
33 Wales. Based on bedform preservation theory, we quantify dune turnover timescales and  
34 hence the magnitude and duration of flow variability, showing that rivers were perennial but  
35 prone to flashy floods lasting 4-16 hours. This disequilibrium bedform preservation is  
36 consistent across 4 Ma of stratigraphy, and coincides with facies-based markers of flooding,  
37 such as mass-preservation of woody debris. We suggest that it is now possible to quantify  
38 climate-driven sedimentation events in the geologic past, and reconstruct discharge  
39 variability from the rock record on a uniquely short (daily) timescale, revealing a formation  
40 dominated by flashy floods in perennial rivers.

## 41 INTRODUCTION

42 Rivers are the most significant drivers of water and sediment transport across the continents<sup>1</sup>,  
43 and associated flood events play a key role in shaping landscapes, impacting ecosystems, and  
44 determining the magnitude, characteristics and locus of sedimentation on the surface of the  
45 Earth<sup>2-10</sup>. In principle, fluvial strata, which constitute a physical record of ancient river  
46 behaviour, provide a key archive to assess the impacts of flooding in the geologic past. An  
47 outstanding research challenge for geoscientists is to decode this archive effectively to  
48 evaluate: how, where and when fluvial deposits may record extreme events; the extent to  
49 which they can be quantified; and how much they may dominate the stratigraphic record<sup>7,11-  
50 13</sup>. This is particularly important as constraints on discharge variability from the geologic  
51 record provide a critical tool to understand past impacts of climate variability on river  
52 behaviour<sup>8,14</sup>. To-date qualitative insights into flow variability have largely been extracted  
53 from the rock record using facies analysis, including observations of super-critical flow  
54 indicators<sup>10,15-19</sup>. However, recent advances in our understanding of fluvial bedform  
55 dynamics in disequilibrium conditions raise the possibility of gaining quantitative insights  
56 into flow variability in ancient rivers<sup>13,20</sup>; when used together with sedimentary observations,  
57 these advances permit reconstruction of flood magnitudes and variability directly from fluvial  
58 stratigraphy.

59 The approach begins with the fundamental morphometrics of fluvial bedforms<sup>20-28</sup>, in  
60 particular dune-scale cross-strata, sub-critical bedforms which are ubiquitous in most ancient  
61 river deposits<sup>20,21,24-26</sup>. Cross-sets are preserved when dunes are not fully reworked by the  
62 prevailing flow, allowing the remaining bedform to become buried (Fig. 1). The “flood

63 hypothesis” of bedform preservation<sup>13</sup> states that enhanced bedform preservation occurs  
64 during floods (especially those with flashy hydrographs) when the formative flood duration,  
65  $T_f$ , is less than the timescale to rework a bedform, known as the turnover timescale,  $T_t$  (Fig. 1,  
66 see Table 1 for definitions). This is due to hysteresis in the adjustment of bedforms to  
67 changing flow conditions, meaning that when  $T_f < T_t$ , bedforms do not have time to adjust in  
68 form to reach equilibrium with the prevailing flow. This key signal of flow variability can be  
69 extracted from dune-scale cross-strata using measurements of the distribution of heights ( $h_{xs}$ )  
70 of preserved dune-scale cross-sets to calculate their coefficient of variation,  $CV$ <sup>13</sup>. In steady-  
71 state flow conditions, which may occur when  $T_f \geq T_t$ , the spread in cross-set heights in  
72 preserved stratigraphy is high: the  $CV$  is expected to be in the range  $0.88 \pm 0.3$  because  
73 existing theory and experiments demonstrate that bedform migration across random bed  
74 topography with low angles of climb, in equilibrium with the prevailing flow, results in low  
75 bedform preservation and high  $CV$  (Fig. 1a)<sup>13,21–23</sup>. In contrast, when preservation occurs in  
76 disequilibrium conditions, which may arise due to flooding, the opposite is true (Fig. 1b). In  
77 this case, limited reworking of sediment within a dune results in lower  $CV$ <sup>26</sup>, with a greater  
78 proportion of the original dune preserved in stratigraphy. Disequilibrium bedform dynamics  
79 have been observed experimentally<sup>29</sup>, and recently dune cross-set  $CV$  has been used to  
80 indicate disequilibrium dynamics in stratigraphy<sup>20,30</sup>. However, flow variability is not the  
81 only origin of disequilibrium conditions: enhanced bedform preservation in disequilibrium  
82 conditions can also be caused by the presence of morphodynamic hierarchy, such as dunes  
83 migrating atop barforms<sup>13,20,26</sup>. Disequilibrium bedform dynamics caused by flow variability  
84 can therefore be difficult to definitively identify in the rock record, due to lack of independent  
85 evidence of variable discharge.

86 Here, we test the flood hypothesis for enhanced bedform preservation in a location where  
87 unambiguous evidence of variable discharge conditions, including mass preservation of  
88 woody debris, can be combined with quantitative bedform and palaeohydrologic analyses.  
89 Therefore, we link for the first time bedform disequilibrium with stratigraphic evidence of  
90 flooding. In doing so, we demonstrate how sophisticated insights into water fluxes, climate  
91 and discharge variability can now be quantified for the geological past from stratigraphic  
92 data.

## 93 Study Area

94 We focus on the Pennant Formation of South Wales, UK (Fig. 2), a 1.3 km thick succession  
95 of Upper Carboniferous (312.4 – 308 Ma, corresponding to the Moscovian age, or Bolsovian-  
96 Asturian substages) fluvial strata<sup>31,32</sup>. The five members of the formation (Llynfi, Rhondda,  
97 Brithdir, Hughes, Swansea) were deposited when South Wales was located near the equator,  
98 at a palaeolatitude of between 2.7°N and 3.0°S<sup>33</sup>. The formation is the product of rivers that  
99 drained the Variscan Mountains, flowing north-west<sup>28</sup> across foreland basin floodplains<sup>34,35</sup>.  
100 The regional climate was warm and wet, with precipitation rates averaging 1.5–5  
101 mm/day<sup>33,36,37</sup>. Individual catchment length and drainage areas reconstructed for multiple  
102 rivers in the Pennant system, based on outcrops in South Wales, average 130-200 km and ~  
103 4500 - 9500 km<sup>2</sup> respectively<sup>28,38,39</sup>. Rapid sedimentation in a foreland basin setting (up to  
104 340 m/Ma)<sup>28,34</sup> resulted in a high-fidelity and high-temporal resolution record of fluvial  
105 processes across a c. 4 myr time period<sup>31,34,35</sup>.

106 The formation comprises bedded, channelised sandstone bodies, with well-preserved  
107 accretion sets and abundant dune-scale cross-bedding<sup>28</sup>. Separating the cliff-forming  
108 sandstone bodies are slope-forming fine-grained sediments representing floodplain  
109 deposition<sup>35</sup>. They contain abundant and well-documented coals<sup>34,40</sup> indicating river  
110 migration across a forested, swampy foreland, characterised by high retention of surface  
111 water. As a result, the Pennant Formation has classically been divided into 3 main facies  
112 associations: fluvial channel, floodplain and mire<sup>34,35</sup> (Supplementary Material S5). These  
113 characteristics are consistent with single-threaded or anastomosing rivers consisting of a few  
114 threads, which have been interpreted as showing perennial discharge regimes<sup>15,28,31,34,35,40,41</sup>.  
115 Qualitative observations of heterolithic deposits at channel margins (Supplementary Material  
116 S5) and the abundance of in-channel plant debris strongly point to the occurrence of flood  
117 events<sup>31,34</sup>, some of which entrained flood plain vegetation. These observations are consistent  
118 with the hypothesis in the thesis of Jones<sup>34</sup>, based on extensive facies analysis across South  
119 Wales, that the Pennant Formation contains evidence of variable discharge conditions. We  
120 therefore exploit this setting, including classical descriptions of facies associations<sup>34,35</sup> as well  
121 as recent reconstructions of palaeo-rivers within the Pennant Formation<sup>28</sup> to compare  
122 numerical and facies evidence of disequilibrium flow conditions related to floods, and in  
123 doing so, quantify discharge variability in a Carboniferous river system for the first time.

## 124 RESULTS

## 125 Quantitative Analysis of Flood Stratigraphy

126 We first consider whether this formation contains quantitative evidence of disequilibrium  
127 bedform preservation, consistent with the flood hypothesis<sup>13</sup>, and if so, what this implies  
128 about flood durations. We then place these results in the context of facies-based evidence of  
129 floods in the form of woody debris accumulations.

130 The mean cross-set height,  $h_{xs}$ , across the Pennant Formation was 0.12 m, with a median of  
131 0.12 m and a standard deviation of 0.06 m (Fig. 3a). Values of maximum height measured  
132 within each cross-set average 0.19 m, and the median grain-size in the formation is  $0.38 \pm$   
133  $0.06$  mm (IQR), i.e., medium-grade sand. Two-tailed Kolmogorov-Smirnov (KS) tests show  
134 that the  $h_{xs}$  distributions of the Pennant Formation's five Members are similar with 99.9%  
135 confidence (Supplementary Material S3h), and Fig. 3a shows that the distributions of mean  
136  $h_{xs}$  follow a similar pattern across all members. This analysis indicates that measured samples  
137 of cross-sets have similar height distributions at member and formation level.

138 Results also show statistically similar low  $CV$  distributions for all members with 90%  
139 confidence with median  $CV$  values spanning 0.36–0.42 (Fig. 3b). The median  $CV$  in the  
140 Pennant Formation is 0.40 and the mean is 0.41. We emphasize that these  $CV$  values are  
141 significantly lower than the theoretical value expected for steady-state bedform preservation  
142 of  $CV = 0.88 \pm 0.3$  (Fig. 4c)<sup>13,21–23</sup>. Indeed, 99.6% of cross-sets have  $CV$  below 0.88, and  
143 96.7% have  $CV$  below 0.58 (0.88–0.3), suggesting that ~97% of dunes measured were  
144 preserved in disequilibrium with the prevailing flow at the time of deposition. These findings  
145 are consistent with theory and observations of disequilibrium (enhanced) bedform  
146 preservation<sup>13,20,25,26</sup> (Fig. 3), and this signal of variable discharge conditions is consistent  
147 across all members of the Pennant Formation (Fig. 3c).

148 These data can be used to quantify bedform turnover timescales,  $T_t$ , and prevailing flood  
149 durations,  $T_f$ . We first explore what our data imply assuming a minimum theoretical bedform  
150 preservation ratio ( $h_{xs}/h_d$ , see Table 1) of 0.3<sup>13,20,26</sup> to obtain estimates of the maximum  
151 durations of  $T_f$  and  $T_t$  (Fig. 4a). Then we evaluate the sensitivity of these results to higher  
152 bedform preservation ratios.

153  $T_t$  calculations (Eq. 3) suggest dunes required a median of 3.2 days to be fully reworked by  
154 flow; similar results are recovered for all members of the Pennant Formation (Fig. 4a).

155 Bedform theory and empirical observations<sup>13</sup> demonstrate dunes preserved in the falling  
156 limbs of flashy floods, in disequilibrium with the prevailing flow, have a bedform  
157 disequilibrium number,  $T^*$ , of  $<1$ , representing the ratio of  $T_f$  and  $T_t$ . When the  $CV$  of cross-  
158 set height is as low as 0.4, as our calculations show,  $T^*$  might be as low as 0.1<sup>13,20</sup>. This  
159 means given the average  $T_t$  of 3.2 days,  $T_f$  is reconstructed as c. 8 hours (0.32 days). Flashy  
160 floods, which can be defined as having abrupt flow deceleration and  $T^* \ll 1$ <sup>13</sup> are often  
161 associated with intense precipitation lasting less than half a day<sup>42</sup> and can have almost  
162 symmetrical hydrographs<sup>15</sup>, so the total length of the average flood preserved in the Pennant  
163 Formation can be approximated as 16 hours. To our knowledge this is the first time flood  
164 durations have been estimated for Carboniferous river systems. Based on paleohydrological  
165 calculations (Table 1 and Methods) we recover median bankfull discharge in individual  
166 channel threads as 140–160 m<sup>3</sup>/s, and considering previous reconstructions of several (i.e. 2-  
167 4) anastomosing threads<sup>28</sup> this could be as high as 640 m<sup>3</sup>/s.

168 Because disequilibrium (enhanced) bedform preservation due to flooding is indicated by our  
169  $CV$  values (Fig. 3), the estimates presented in Fig. 4a are conservative maxima. The bedform  
170 preservation ratio,  $h_{xs}/h_d$ , is the ratio of measured mean cross-set height to estimated mean  
171 original dune height, and is influenced by the equilibrium dynamics of flow. Steady state  
172 dynamics are implicit in many bedform scaling relations<sup>22</sup>, assuming  $h_{xs}/h_d = 0.3$ , however  
173 plausible non-steady state values of  $h_{xs}/h_d$  may be as great as 0.6, based on theory and  
174 experiments which show enhanced preservation during the falling limbs of flashy floods<sup>13,20</sup>.  
175 As  $h_{xs}/h_d$  increases from 0.3 to 0.6 for a known  $h_{xs}$  (0.12 m on average for the Pennant  
176 Formation), the median  $T_t$  reduces from 3.2 days to 0.9 days (Fig. 5a). This means that while  
177 the falling limb of floods may be as long as 8 hours assuming a ‘typical’ bedform  
178 preservation ratio of 0.3,  $T_f$  could be as short as 2 hours assuming a bedform preservation  
179 ratio as large as 0.6. Durations are unlikely to be shorter than this as we do not see complete  
180 dunes preserved. The shaded regions in Fig. 5 illustrate the plausible range in  
181 palaeohydrologic parameters, with bankfull discharges for individual channels reconstructed  
182 from cross-set heights as between 88 and 160 m<sup>3</sup>/s (Fig. 5b). These could represent lower  
183 limits on bankfull discharge, with rare gravel-grade dunes suggesting discharges a factor of  
184 1.5 – 2 greater than the sand fraction in the Pennant Formation<sup>28</sup>, although independent  
185 architectural constraints on channel morphology result in comparable discharge  
186 reconstructions, with a median of 140 m<sup>3</sup>/s per channel.<sup>28</sup>

187 Finally, we note that the flow intermittency factor of a river,  $I_f$ , can be used to obtain  
188 quantitative context into annual flow regime, and can be visualised as the proportion of the  
189 year a river would need to maintain bankfull discharge conditions to equal an estimate of the  
190 yearly water budget. For ancient fluvial systems such as the Pennant Formation,  $I_f$  can be  
191 estimated using published constraints on palaeogeographic and palaeo-precipitation rates (see  
192 Methods) to obtain a plausible annual water budget, and we exploit these to obtain first-order  
193 estimates of water flow intermittency factors for Pennant rivers. By comparing these  
194 constraints on mean annual discharge to our bankfull estimates (Fig. 4b), we estimate  $I_f =$   
195 0.17 – 0.44 (see Methods). This suggests that if the rivers of the Pennant Formation sustained  
196 bankfull conditions they could complete annual discharge in 62 – 160 days, which is  
197 consistent with perennial river systems, as discussed further below.

### 198 **Facies-based evidence for flooding**

199 The quantitative analysis above, based on bedform theory, indicates that sediment deposition  
200 in the palaeo-rivers of the Variscan Foreland was controlled by disequilibrium bedform  
201 dynamics, which we relate to floods that had durations up to 16 hours. But to what extent are  
202 these quantitative conclusions supported by facies-based observations? Fluvial channel  
203 facies in the Pennant Formation can be divided into 3 major lithofacies (*conglomerate*,  
204 *sandstone* and *heterolithic*) after Jones and Hartley<sup>35</sup> which have been well-documented since  
205 the 1960s, and for which variable discharge conditions have been qualitatively suggested.  
206 We do not repeat these analyses but focus on the *conglomerate lithofacies*, first described by  
207 Jones and Hartley<sup>35</sup> as conglomerates in which the clasts often comprise plant debris. We  
208 present new observations of woody debris, below, which we link to our quantitative  
209 approach. Further contextual details on facies that have been observed in the Pennant  
210 Formation<sup>34</sup> are presented in the supplementary material (S5).

211 Dense accumulations of fossilised plant materials, or “plant conglomerates”<sup>35</sup>, are abundant  
212 and well-documented in the Pennant Formation. Plant fossils are preserved as a mixture of  
213 coalified compactions, compressions, as casts with well-preserved surface features, and  
214 occasional perimineralization. Identifiable fossils are mostly genus *Calamites* and  
215 *Lepidodendron*. *Calamites*, a genus of arborescent Equisetales (horsetails), grew in rapidly  
216 shifting and aggrading riparian settings<sup>43</sup>, proximal to channels, inhabiting levees, bars, and  
217 overhanging river channels. *Calamites* grew to its full height within 2 seasons, whereas  
218 *Lepidodendron* grew further from river channels, requiring more established substrate before

219 reaching ~35 m in height and developing woody branches after 5 – 10 years of  
220 growth<sup>31,41,44,45</sup>. Although ubiquitous throughout the Pennant Formation, the densest plant  
221 accumulations (Fig. 6), historically referred to as “conglomerates”<sup>35</sup> are observed in this  
222 study at 6 localities (Supplementary Material S3), but are documented throughout the  
223 formation<sup>31,34,35,41,46</sup>. They are characterised by large volumes of woody debris preserved at  
224 the bases of channel packages and accretion sets (Supplementary Material S7), only  
225 containing gravel-grade lithic clasts in a few rare instances. Conglomeratic debris beds are  
226 0.25 – 3 m in thickness, and contain mostly *Lepidodendron* preserved as casts and  
227 compactions at varied stages of surface degradation. Fossils overlap and interlock, and occur  
228 in a matrix of highly macerated vegetation mixed with sand and organic-rich mud and silt.  
229 The *conglomerate lithofacies* contains a higher proportion of large debris fossils than the  
230 *sandstone lithofacies* (Supplementary Material S5), and associated sediment is often poorly  
231 organised, but may contain a range of bedforms, from high-angle dune-scale cross  
232 stratification to upper plane-bed lamination. No in-situ plant fossils (e.g. stumps) are  
233 observed.

234 The maximum length of woody debris we observed is 250 cm, with a median of 13 cm (Fig.  
235 6f). The maximum reconstructed cylindrical volume of plant debris is 95,000 cm<sup>3</sup> with a  
236 median of 237 cm<sup>3</sup>. While these woody debris accumulations have not before been linked  
237 with palaeohydrological observations, KS tests (see Methods and S3, 4) demonstrate that  
238 dune cross-sets, where found in close association with woody debris in the *conglomerate*  
239 *lithofacies*, have an even lower *CV* than those documented elsewhere (Fig. 3) with 90%  
240 confidence. This shows that, whilst bedform preservation for sandy channel deposits is  
241 enhanced consistently at formation level, even greater enhancement is observed where debris-  
242 dominated facies associations are present. These data suggest that disequilibrium bedform  
243 preservation prevailed throughout the Pennant Formation and was particularly enhanced in  
244 flow associated with preservation of woody debris.

245 We interpret the observed debris conglomerates as log-jam deposits, generated by floods.  
246 First, the characteristics of the log-jam deposits observed here are similar to modern and  
247 ancient examples<sup>10,16,46–49</sup>, where debris orientation, sorting, and palaeobiology are  
248 comparable. Once plant material is in the river channel, log-jams can occur due to obstacles  
249 or flow separation between large objects such as bars or entire tree trunks<sup>50</sup>. Therefore,  
250 secondly, the formation of log-jams in the palaeo-rivers of the Variscan foreland is feasible



251 due to the known presence of barforms and because *Lepidodendron* grew large enough to act  
252 as *key members* in log-jams<sup>43</sup>. Further, log-jams are known to have been frequent and  
253 diverse in Carboniferous rainforests<sup>43</sup>, and in ancient alluvial systems<sup>4,10,16,49,50</sup>. Moreover,  
254 The classic observations of Jones<sup>34</sup> document woody debris up to 10 m long, suggesting the  
255 presence of material large enough to generate a significant obstruction in the channel<sup>43</sup>. We  
256 suggest, therefore, that the deposits observed represent transport jams as described by Gibling  
257 et al.<sup>43</sup> and we link these events to the discharge variability documented using our  
258 quantitative bedform approach.

## 259 **DISCUSSION**

### 260 ***Bedform disequilibrium***

261 Based on our quantitative bedform analysis, we document a *CV* of dune-scale cross-set height  
262 distributions in the Pennant Formation of  $0.40 \pm 0.07$  (IQR) found throughout the unit (Fig.  
263 3), which demonstrates that stratigraphy in the Pennant Formation preserves non-steady-state  
264 bedform dynamics. This is coupled with clear evidence for variable discharge conditions and  
265 the occurrence of floods. We show that 97% of observed cross-sets ( $N = 271$ ) possess low  
266 *CV* (classified as  $\leq 0.88 \pm 0.3$ ) consistent with enhanced dune preservation, and this appears  
267 to be the norm across up to 1.3 km of stratigraphy, a significant interval representing 4 Ma of  
268 deposition. Enhanced bedform preservation is being increasingly recognised in ancient fluvial  
269 systems<sup>20,30</sup>. Uniquely, our work in the Pennant Formation also links this signature to facies-  
270 based observations of flood-driven woody debris entrainment and deposition, and we  
271 interpret these disequilibrium conditions to likely reflect the prevailing flow during the falling  
272 limbs of floods. Based on bedform turnover timescale calculations, we reconstructed falling  
273 limb flood durations ( $T_f$ ) of 2–8 hours, suggesting that relatively flashy floods had a total  
274 duration 4–16 hours, with bankfull discharges of 140–160 m<sup>3</sup>/s per channel thread. This  
275 duration is consistent with published estimates of catchment size, with flow estimated to  
276 propagate through a catchment typical of the outcrops studied in 12 – 40 hours<sup>28</sup>  
277 (Supplementary Material S4). This is the first time that dune bedform-based analyses of  
278 variable discharge conditions have been used to constrain flood durations in the ancient past.  
279 In conjunction with facies-based approaches, discussed below, this methodology provides a  
280 new way of quantifying the magnitude and duration of floods in the stratigraphic record.

### 281 ***Woody debris***

282 We present evidence of log-jams and woody debris accumulations throughout the Pennant  
283 Formation, and we interpret these to have formed during floods, such as those that we  
284 quantify above. Rapid sedimentation and high-fidelity surface preservation of fossils in the  
285 *conglomerate lithofacies*, as well as their poor sorting and significant volume, speaks to high-  
286 magnitude storm-driven events. Plant accumulations including woody and peaty debris in  
287 accretion packages in other facies associations<sup>35</sup> (e.g., the *sandstone lithofacies*,  
288 Supplementary Material S5) can also be explained by high-discharge events. These deposits  
289 are ubiquitous in the formation and occur in every member, implying rivers that were prone  
290 to discharge variability in a tropical ever-wet rainforest setting.

291 While plant material can be recruited into river channels by direct abscission, wind-blown  
292 input, and undercutting and collapse of the banks<sup>54</sup>, we suggest that the woody debris  
293 conglomerates present strong evidence of overbank flooding: firstly, the volume and density  
294 of many of the conglomeratic beds speak to the rapid recruitment of vegetation from large  
295 areas of forested floodplain, especially when considering estimates on Carboniferous tree  
296 spacing<sup>51,52</sup>. Secondly, the abundance of comminuted plant material gives insight into  
297 formation mechanism, implying maceration during transport, or prior decomposition on the  
298 forest floor. When found amongst large samples of woody debris this either requires flood  
299 water to transport rotted vegetation from the floodplain or to macerate fresh vegetation in  
300 high-energy flow. Further, these deposits are poorly sorted, with the lengths of measurable  
301 debris fossils in the 5 - 95% range being 0.03 – 1 m. It is unlikely this could be caused by  
302 gradual build-up of logs on/adjacent to a barform, and instead suggests rapid accumulation in  
303 a high energy setting. Third, the high quality of preservation of many fossils suggests rapid  
304 sedimentation, occurring during high and falling stages of flood events<sup>50</sup>.

305 Incremental floodplain cannibalisation is not favoured in this interpretation of log-jam debris  
306 recruitment not only due to the large volume of the deposits, but also due to the  
307 disproportionate absence of fossilised plant roots. If vegetation was recruited by bank  
308 collapse, this would place the entire tree, including roots, into the channel. However, these  
309 deposits do not contain roots, but mostly branches of *Lepidodendron*, which must have been  
310 collected by overbank flow where these organisms grew. *Lepidodendron* grew relatively far  
311 from river channels, requiring at least 5-10 years of stable growth before generating  
312 branches<sup>53,54</sup>, so it is unlikely that large volumes of branch material would have been  
313 recruited directly from the river bank. Furthermore, the absence of any in-situ tree fossils

314 suggests woody material was not sourced from plants living within the channel, consistent  
315 with palaeohydrologic reconstructions of these systems<sup>28</sup> that show they were perennial.  
316 Palaeohydrological reconstructions show rivers channels were no wider than 200 m. Bank  
317 collapse on a scale large enough to incorporate enough of the floodplain into the channel to  
318 potentially cause a log-jam is therefore unlikely, and only occurs in the largest rivers today<sup>55–</sup>  
319 <sup>58</sup>. Even if undercutting and bank collapse were an additional mechanism, this process occurs  
320 especially during floods<sup>43,50,59</sup>.

321 Together, our quantitative analyses, coupled with our observations of log-jam deposits, show  
322 that disequilibrium conditions related to variable discharge and flooding are ubiquitous across  
323 1.3 km of Welsh Carboniferous stratigraphy. Our data are unique in the ability to link  
324 qualitative facies indicators of potential discharge variability to quantitative evidence of  
325 enhanced bedform preservation. Where woody debris is found in the densest concentrations  
326 (i.e., log-jam deposits in the *conglomerate lithofacies* and plant-rich beds in the *sandstone*  
327 *lithofacies*), it coincides with lower cross-set *CV* to 90% confidence (Fig. 3b). Almost all  
328 cross-sets measured across the formation indicate disequilibrium preservation, interpreted to  
329 be driven by flashy floods, however, dunes shown to have occurred in stratigraphic proximity  
330 to debris-transporting flood events are preserved with the lowest *CV* values. This  
331 demonstrates that debris accumulations record the same high-discharge events that are  
332 recorded by the disequilibrium preservation of dunes in ancient rivers, establishing dune  
333 cross-set *CV* as a robust indicator of discharge variability. This also highlights the critical  
334 importance of uniting facies-based evidence of variable discharge conditions with  
335 quantitative insights from bedform theory.

### 336 ***Discharge regimes***

337 A number of indicators have been developed to identify systems with high discharge  
338 variability in the geologic record<sup>10,15,16,60</sup>, including Froude transcritical or supercritical  
339 structures and evidence of long periods free of discharge (e.g. *in-situ* vegetation), often  
340 associated with strong seasonal precipitation patterns. However, facies evidence indicates that  
341 rivers had persistent discharge<sup>61</sup> rather than strongly seasonal or highly intermittent discharge  
342 patterns<sup>10,15,16,28,34,35</sup>, consistent with our quantitative calculations. In the Pennant Formation  
343 trans- or supercritical sedimentary structures have been rarely observed, as sedimentation is  
344 dominated by sub-critical dune bedforms alongside occasional upper plane bed lamination in  
345 close association with woody debris. Moreover, supercritical conditions are not expected in

346 these rivers given their reconstructed morphodynamics and flow velocities (see also  
347 Supplementary Material S5). The abundance and diversity of plants in upper Carboniferous  
348 coal forests implies that vegetation would colonise the river channel if long periods free of  
349 discharge occurred. However, no *in-situ* vegetation has been observed in this formation,  
350 leading to the inference that rivers were perennial<sup>15,16</sup>. Moreover, the Pennant Formation's  
351 fluvial channel facies contains abundant well-developed accretion sets, characteristic of  
352 perennial river deposits, as opposed to streams supplied largely by seasonal  
353 precipitation<sup>15,17,18,62–65</sup>. Serinaldi et al.<sup>66</sup> also note that monsoonal regimes are typically  
354 characterized by sustained floods (5–25 days).  $T_t$  calculations, on the other hand, yield flood  
355 durations less than 1 day, which is inconsistent with models of subtropical systems, but  
356 consistent with flashy, precipitation- (storm-) driven floods in a perennial system. Further,  
357 Leary and Ganti<sup>13</sup> found that sustained floods may have sufficiently long recession periods  
358 that bedforms reach equilibrium with the flow, in contrast with our results showing  
359 disequilibrium bedform preservation. All of these factors point towards a system not  
360 dominated by strong seasonality, but instead by storm precipitation on a daily timescale.

361 Finally, estimates of the water flux intermittency factor,  $I_f$ , reconstructed for the Pennant  
362 Formation of 0.17 to 0.44 (methodology) are not consistent with ephemeral discharge  
363 rivers<sup>20,27</sup> but suggest the total annual water budget could be completed if bankfull conditions  
364 were sustained for around 1/3 of the year. The dominant grain-size, abundance of vegetation  
365 and perhumid climate is also potentially analogous to fluvial-dominated channels of the  
366 Mahakan Delta, Indonesia<sup>67</sup>. The intermittency factors we obtain are therefore broadly  
367 characteristic of perennial but variable flow in sand-bedded rivers<sup>68</sup>.

### 368 ***Stratigraphic completeness***

369 One final implication of the low  $CV$  values for fluvial cross-sets documented in this study is  
370 that they imply elevated bedform preservation ratios. Consequently, the palaeohydrological  
371 and facies-based results of this study show the “unusual completeness”<sup>11</sup> of the strata (in  
372 terms of bedform preservation) is likely due to discharge variability related to flooding<sup>13,15,28</sup>.  
373 This conclusion raises important questions about preservation of flow events in the  
374 stratigraphic record<sup>11,21</sup>. Variscan tectonics and associated accommodation generation  
375 undoubtedly contributed to the high rates of alluvial aggradation, as well as the preservation  
376 of woody debris<sup>4</sup>. However, given that almost the entire Pennant Formation contains the  
377 signature of disequilibrium bedform preservation, steady-state flow conditions appear to be

378 disproportionately underrepresented. One explanation is that river sediment may behave in a  
379 state of disequilibrium more often than not due to the known hysteresis between flow  
380 conditions and adjusting dune morphology<sup>69</sup>. If this is true for the Pennant Formation, then  
381 this study offers further evidence that ancient rivers should not be treated as binary – either at  
382 steady-state or non-steady-state – but that disequilibrium bedform preservation is occurring  
383 regularly due to constant discharge variability.

384 However, given that we have extensive facies-based evidence for flood discharge conditions,  
385 our observations (e.g. Fig. 6) provide clear evidence for significant changes in flow  
386 conditions. Floods occurred over brief timescales, as we quantify above, therefore leaving  
387 perennial flow states to dominate the annual hydrograph, but evidently not the sedimentary  
388 record. In this scenario, the finding that 97% of observed cross-sets show *CV* values  
389 consistent with flood-driven discharge variability implies the exclusion of the vast majority of  
390 geologic time from the depositional record<sup>11</sup>. This study provides bedform-based evidence of  
391 disequilibrium flow conditions driven by flashy, storm-driven flooding, which we are able to  
392 link unambiguously with independent evidence of ancient floods for the first time, and adds  
393 to growing evidence that many systems may dominantly preserve sediment under conditions  
394 of bedform disequilibrium<sup>20,29,30</sup>. Consequently, we are able to reconstruct the signature of  
395 discharge variability on a daily timescale and our work illustrates how quantitative bedform  
396 analyses increasingly enable flood characteristics to be recovered from the rock record.

397 Taken together, these results demonstrate vividly how a careful combination of bedform and  
398 facies-based approaches can unlock fresh insights into Earth's surface sedimentary systems  
399 and surface processes. This study represents the first quantitative investigation of bedform  
400 dynamics in upper Carboniferous palaeo-rivers and show how preserved bedforms can be  
401 used to extract signals of ancient discharge variability from fluvial stratigraphy.

402 Palaeohydrological reconstructions reveal that the sand-bedded perennial palaeo-rivers in the  
403 Variscan foreland of the UK were significantly influenced by precipitation-driven flood  
404 variability, the signature of which dominated stratigraphy over a period of 4 Ma. Floods had  
405 duration 4–16 hours, causing enhanced preservation of dunes and recruiting large volumes of  
406 woody debris, sometimes as log jams, and flood discharges had magnitudes of 140–160 m<sup>3</sup>/s  
407 for individual channel threads.

## 408 **METHODS**

409 **Field observations**

410 Primary data were collected in Autumn 2021 and Spring 2022 across 20 sites in the South  
411 Wales and Pembrokeshire Coalfields (Figure 2; Supplementary Materials S1, S2) from the  
412 five Members of the Pennant Formation. Primary data included cross-set height distributions  
413 (Fig. 7a, b), the geometries of various architectural elements (Fig. 7c, d), grain-size, and  
414 observations of flood facies (Fig. 6).

415 Cross-set height distributions were collected following the sampling strategy of Lyster et al<sup>20</sup>,  
416 Ganti et al<sup>24</sup> and are explained in detail by Wood et al<sup>28</sup>. Cross-set bounding surfaces were  
417 first identified, and cross-set height was measured (to a precision of  $\pm 5$  mm) at regular  
418 intervals, with between 7 and 61 measurements per cross-set. We used cross-bed dip  
419 directions, palaeoflow estimates (both regional and local) and 3D outcrops with more than  
420 one exposed plane to ensure we sampled the cross-set parallel to the migration direction. A  
421 total of 4390 height measurements were taken across 271 cross-sets (Table S2).

422 Measurements of maximum cross-set height (with sample size  $N = 1735$ ) were also collected  
423 separately. Relationships were established between the maximum and mean height from the  
424 recorded distributions (Table S2), allowing estimation of mean  $h_{xs}$  from cross-sets where only  
425 the maximum value was measured. This increased the sample size of mean cross-set heights  
426 to  $N = 6125$ . For each observed cross-set, the grain-size of the sediment was also established  
427 (see S4: Extended Methodology, for more detail). The geometries of architectural elements,  
428 including the dimensions of channel and accretion packages, were measured using a Haglof  
429 Laser Geo laser range finder to a precision of  $\pm 5$  cm. Data on woody debris fossils were  
430 collected by measuring their long and short axis to a precision of  $\pm 5$  mm, and their location  
431 within the stratigraphic architecture was recorded.

432 **Quantitative palaeohydrology**

433 Fundamental to the “flood hypothesis”<sup>26</sup> is the detection of enhanced bedform preservation in  
434 fluvial strata. Measured  $h_{xs}$  distributions were used to calculate the coefficient of variation of  
435 cross-set height,  $CV$ , where:

436

437

$$CV = \frac{\sigma}{\mu}$$

438 *Eq. 1*

439 in which  $\sigma$  is the standard deviation and  $\mu$  is the mean of the cross-set heights within a single  
440 cross-set. The  $CV$  reflects the preservation of the original dune, and therefore the equilibrium  
441 dynamics of flow: a  $CV$  of 0.88 is expected in equilibrium conditions<sup>21–23</sup> and  $CV$  decreases  
442 as bedform preservation becomes enhanced (Fig. 1).

443 To calculate the original dune height from cross-sets observed in the field, the relationship  
444 established by Leclair and Bridge<sup>22</sup> was used, based on previous theoretical work<sup>21</sup>:

445

$$h_d = 2.9(\pm 0.7)h_{xs}$$

446 *Eq. 2*

447 where  $h_d$  is the mean original dune height, and  $h_{xs}$  is the mean cross-set height. Values of  $h_d$   
448 were then used in an array of further palaeohydrological calculations to build a complete  
449 picture of river morphodynamics. See Supplementary Material (S4) for further detail on  
450 palaeohydrologic calculations and uncertainty.

451 To estimate uncertainty, Monte Carlo uncertainty propagation was used to generate a  
452 distribution of values for  $h_d$  that reflects the true spread of the data, following previous  
453 hydrological studies<sup>20,27,70</sup>. For Equation 2,  $10^6$  random samples were generated between  
454 bounds defined by  $\mu - \sigma$  and  $\mu + \sigma$  where  $\mu$  is the mean and  $\sigma$  is one standard deviation. This  
455 was repeated for all formulae with a stated error, and propagated uncertainties were carried  
456 through.

457 Bedform turnover timescale ( $T_t$ ) is defined as the time to displace the volume per unit width  
458 of sediment in a bedform, i.e., the length of time required for a bedform to be completely  
459 reworked by the prevailing flow<sup>12</sup>. This parameter is used to indicate whether bedforms

460 evolved in equilibrium with the prevailing flow, as a  $T_t$  that is greater than the duration of the  
461 prevailing flow,  $T_f$ , implies a hysteresis that results in limited reworking of the bedform. This  
462 study determines  $T_t$  using the methods of Myrow et al<sup>12</sup> and Martin and Jerolmack<sup>69</sup>, in  
463 which:

$$464 \quad T_t = \frac{\lambda h_d \beta}{q_b}$$

465 *Eq. 3*

466 where  $\lambda$  is dune wavelength (approximated as  $\lambda = 7.3H$ , where  $H$  is the formative flow depth),  
467 the shape factor  $\beta \approx 0.55$  and  $q_b$  is the unit bedload flux (See Supplementary Material S4).

468 Myrow et al<sup>12</sup> define a dimensionless bedform disequilibrium number,  $T^*$ :

$$469 \quad T^* = \frac{T_f}{T_t}$$

470 *Eq. 4*

471 Using data compiled from experiments and modern rivers by Leary and Ganti<sup>13</sup>, it is possible  
472 to establish plausible values of  $T^*$  for calculated values of  $CV$ . Their results imply that dunes  
473 preserved in disequilibrium with falling-limb flood discharge lead to cross-sets low values of  
474  $CV$  and  $T^*$ . Based on their data, we take 0.1 as a plausible value of  $T^*$ , meaning  $T_f = 0.1T_t$ .

475 The flow intermittency factor,  $I_f$ , is defined as the fraction of the total time in which bankfull  
476 flow would accomplish the same amount of water discharge as the real hydrograph<sup>68</sup>:

$$477 \quad I_f = \frac{\sum Q(t)}{Q_{bf} \sum t}$$

478 *Eq. 5*

479 where  $\sum Q(t)$  is the sum of the time dependent discharge (i.e., the unit discharge),  $Q_{bf}$  is the  
480 discharge at bankfull conditions and  $\sum t$  is the timespan. Flow intermittency requires  
481 estimation of a yearly water budget, and this necessitates a range of assumptions. Based on  
482 atmospheric general circulation models<sup>33,36</sup>, the palaeo-precipitation rate was estimated as  
483 between 1.5 and 2.5 mm/day, and catchment area has been estimated by Wood et al<sup>28</sup> as 4500  
484 - 9500 km<sup>2</sup>, based on catchment scaling relationships<sup>39</sup> and previously published



485 palaeogeographic constraints<sup>32</sup>. Multiplying the annual average precipitation rate by the  
486 catchment area gives an estimate of the discharge (m<sup>2</sup>/s) supplied to the catchment, once  
487 modified to account for infiltration and evaporation of 20%<sup>71</sup> (Supplementary Material S4).

#### 488 **Statistical tests**

489 Two-tailed Kolomogorov-Smirnov (KS) tests were performed in order to test the similarity of  
490 datasets, with the null hypothesis that the tested datasets have similar distributions. Firstly,  
491 the  $h_{xs}$  data collected in each member were tested against each other and against the data  
492 collected from the Pennant Formation as a whole. Secondly, the same tests were conducted  
493 for the cross set *CV*. Finally, the *CV* values of cross-sets associated with woody debris were  
494 tested against those not associated with debris. See S3h, S3i and S3j in the Supplementary  
495 Materials, respectively, for these statistical tests.

#### 496 **DATA AVAILABILITY**

497 All data generated in this study are available in the Supplementary Materials and have been  
498 deposited in the Figshare database [doi:10.6084/m9.figshare.22564942,  
499 doi:10.6084/m9.figshare.22811333]

#### 500 **REFERENCES**

- 501 Milliman, J. D. & Meade, R. H. Worldwide delivery of river sediment to the oceans. *Geology*  
502 **91**, 1–21 (1983).
- 503 Baker, V. R., Kochel, R. C. & Patton, P. C. *Flood Geomorphology*. (Wiley-Interscience,  
504 1988).
- 505 Parsons, M., McLoughlin, C. A., Kotschy, K. A., Rogers, K. H. & Rountree, M. W. The  
506 effects of extreme floods on the biophysical heterogeneity of river landscapes. *Frontiers in*  
507 *Ecology and the Environment* **3**, 487–494 (2009).
- 508 Trümper, S. *et al.* Late Palaeozoic red beds elucidate fluvial architectures preserving large  
509 woody debris in the seasonal tropics of central Pangaea. *Sedimentology* **67**, 1973–2012  
510 (2020).
- 511 Palik, B. *et al.* Geomorphic variation in riparian tree mortality and stream coarse woody  
512 debris recruitment from record flooding in a coastal plain stream. *Écoscience* **5**, 551–560  
513 (2016).
- 514 Comiti, F., Lucía, A. & Rickenmann, D. Large wood recruitment and transport during large  
515 floods: A review. *Geomorphology* **269**, 23–39 (2016).
- 516 Whittaker, A. C. *et al.* Flood variability in the rock record? Disequilibrium bedform  
517 preservation in ancient fluvial stratigraphy. in *EGU General Assembly, Vienna, Austria, 23-*  
518 *27 May 2022, EGU-6440* (2022).

519 Watkins, S. E. *et al.* Are landscapes buffered to high-frequency climate change? A  
520 comparison of sediment fluxes and depositional volumes in the Corinth Rift, central Greece,  
521 over the past 130 k.y. *GSA Bulletin* **131**, 372–388 (2018).

522 Romans, B. W., Castelltort, S., Covault, J. A., Fildani, A. & Walsh, J. P. Environmental  
523 signal propagation in sedimentary systems across timescales. *Earth Sci Rev* **153**, 7–29 (2016).

524 Fielding, C. R., Alexander, J. & Allen, J. P. The role of discharge variability in the formation  
525 and preservation of alluvial sediment bodies. *Sediment Geol* **365**, 1–20 (2018).

526 Paola, C., Ganti, V., Mohrig, D., Runkel, A. C. & Straub, K. M. Time Not Our Time:  
527 Physical Controls on the Preservation and Measurement of Geologic Time. *Annual Review of*  
528 *Earth and Planetary Sciences* **46**, 409–438 (2018).

529 Myrow, P. M., Jerolmack, D. J. & Perron, J. T. Bedform disequilibrium. *Journal of*  
530 *Sedimentary Research* **88**, 1096–1113 (2018).

531 Leary, K. C. P. & Ganti, V. Preserved Fluvial Cross Strata Record Bedform Disequilibrium  
532 Dynamics. *Geophys Res Lett* **47**, (2020).

533 Colombera, L., Arévalo, O. J. & Mountney, N. P. Fluvial-system response to climate change:  
534 The Paleocene-Eocene Tresp Group, Pyrenees, Spain. *Glob Planet Change* **157**, 1–17  
535 (2017).

536 Plink-Björklund, P. Morphodynamics of rivers strongly affected by monsoon precipitation:  
537 Review of depositional style and forcing factors. *Sediment Geol* **323**, 110–147 (2015).

538 Fielding, C. R., Allen, J. P., Alexander, J. & Gibling, M. G. Facies model for fluvial systems  
539 in the seasonal tropics and subtropics. *Geology* **37**, 623–626 (2009).

540 Adams, M. M. & Bhattacharya, J. P. No change in fluvial style across a sequence boundary,  
541 Cretaceous Blackhawk and Castlegate formations of central Utah, U.S.A. *Journal of*  
542 *Sedimentary Research* **75**, 1038–1051 (2005).

543 Chamberlin, E. P. & Hajek, E. A. Using bar preservation to constrain reworking in channel-  
544 dominated fluvial stratigraphy. *Geology* **47**, 531–534 (2019).

545 McMahan, W. J. & Davies, N. S. High-energy flood events recorded in the Mesoproterozoic  
546 Meall Dearg Formation, NW Scotland; their recognition and implications for the study of  
547 pre-vegetation alluvium. *J Geol Soc London* **175**, 13–32 (2018).

548 Lyster, S. J., Whittaker, A. C., Hajek, E. A. & Ganti, V. Field evidence for disequilibrium  
549 dynamics in preserved fluvial cross-strata: A record of discharge variability or  
550 morphodynamic hierarchy? *Earth Planet Sci Lett* **579**, (2022).

551 Paola, C. & Borgman, L. Reconstructing random topography from preserved stratification.  
552 *Sedimentology* **38**, 553–565 (1991).

553 Leclair, S. F. & Bridge, J. S. Quantitative interpretation of sedimentary structures formed by  
554 river dunes. *Journal of Sedimentary Research* **71**, 713–716 (2001).

555 Leclair, S. F. Preservation of cross-strata due to the migration of subaqueous dunes: an  
556 experimental investigation. *Sedimentology* **49**, 1157–1180 (2002).

557 Ganti, V., Whittaker, A. C., Lamb, M. P. & Fischer, W. W. Low-gradient, single-threaded  
558 rivers prior to greening of the continents. **116**, 11652–11657 (2019).

559 Leary, K. & Buscombe, D. Estimating Sand Bedload in Rivers by Tracking Dunes: a  
560 comparison of methods based on bed elevation time-series. *Earth Surface Dynamics*  
561 *Discussions* **8**, 161–172 (2019).

562 Ganti, V., Hajek, E. A., Leary, K., Straub, K. M. & Paola, C. Morphodynamic Hierarchy and  
563 the Fabric of the Sedimentary Record. *Geophys Res Lett* **47**, (2020).

564 Lyster, S. J. *et al.* Reconstructing the morphologies and hydrodynamics of ancient rivers from  
565 source to sink: Cretaceous Western Interior Basin, Utah, USA. *Sedimentology* **68**, 2854–2886  
566 (2021).

- 567 Wood, J., McLeod, J. S., Lyster, S. J. & Whittaker, A. C. Rivers of the Variscan Foreland:  
568 fluvial morphodynamics in the Pennant Formation of South Wales, UK. *Journal of the*  
569 *Geological Society* (2022) doi:<https://doi.org/10.31223/X5TK94>.
- 570 Jerolmack, D. J. & Mohrig, D. Frozen dynamics of migrating bedforms. *Geology* **33**, 57–60  
571 (2005).
- 572 Cardenas, B. T. *et al.* The anatomy of exhumed river-channel belts: Bedform to belt-scale  
573 river kinematics of the Ruby Ranch Member, Cretaceous Cedar Mountain Formation, Utah,  
574 USA. *Sedimentology* **67**, 3655–3682 (2020).
- 575 Falcon-Lang, H. J., Cleal, C. J., Pendleton, J. L. & Wellman, C. H. Pennsylvanian (mid/late  
576 Bolsovian-Asturian) permineralised plant assemblages of the Pennant Sandstone Formation  
577 of southern Britain: Systematics and palaeoecology. *Rev Palaeobot Palynol* **173**, 23–45  
578 (2012).
- 579 Burgess, P. M. & Gayer, R. A. Late Carboniferous tectonic subsidence in South Wales:  
580 implications for Variscan basin evolution and tectonic history in SW Britain. *J Geol Soc*  
581 *London* **157**, 93–104 (2000).
- 582 Tabor, N. J. & Poulsen, C. J. Palaeoclimate across the Late Pennsylvanian–Early Permian  
583 tropical palaeolatitudes: A review of climate indicators, their distribution, and relation to  
584 palaeophysiographic climate factors. *Palaeogeogr Palaeoclimatol Palaeoecol* **268**, 293–310  
585 (2008).
- 586 Jones, C. M. The sedimentology of Carboniferous fluvial and deltaic sequences; the Roaches  
587 Grit Group of the South-West Pennines and the Pennant Sandstone of the Rhondda Valleys.  
588 (Keele University, 1977).
- 589 Jones, J. A. & Hartley, A. J. Reservoir characteristics of a braid-plain depositional system:  
590 the Upper Carboniferous Pennant Sandstone of South Wales. *Geological Society Special*  
591 *Publications* **73**, 143–156 (1993).
- 592 Peyser, C. E. & Poulsen, C. J. Controls on Permo-Carboniferous precipitation over tropical  
593 Pangaea: A GCM sensitivity study. *Palaeogeogr Palaeoclimatol Palaeoecol* **268**, 181–192  
594 (2008).
- 595 Sombroek, W. Spatial and temporal patterns of Amazon rainfall. Consequences for the  
596 planning of agricultural occupation and the protection of primary forests. *Ambio* **30**, 388–396  
597 (2001).
- 598 Nyberg, B. *et al.* Revisiting morphological relationships of modern source-to-sink segments  
599 as a first-order approach to scale ancient sedimentary systems. *Sediment Geol* **373**, 111–133  
600 (2018).
- 601 Hack, J. T., Seaton, F. A. & Nolan, T. B. *Studies of Longitudinal Stream Profiles in Virginia*  
602 *and Maryland. United States Department of the Interior* (1957).
- 603 Jenkins, B. H. J. The sequence and correlation of the coal measures of Pembrokeshire.  
604 *Quarterly Journal of the Geological Society* **118**, 65–101 (1961).
- 605 Cleal, C. J. & Thomas, B. M. *Plant fossils of the British Coal Measures*. (The  
606 Palaeontological Association, 1994).
- 607 Brunner, M. I. *et al.* Flood type specific construction of synthetic design hydrographs. *Water*  
608 *Resour Res* **53**, 1390–1406 (2017).
- 609 Gibling, M. R., Bashforth, A. R., Falcon-Lang, H. J., Allen, J. P. & Fielding, C. R. Log jams  
610 and flood sediment buildup caused channel abandonment and avulsion in the pennsylvanian  
611 of atlantic Canada. *Journal of Sedimentary Research* **80**, 268–287 (2010).
- 612 Thomas, B. A. & Cleal, C. J. Arborecent lycophyte growth in the late Carboniferous coal  
613 swamps. *Source: The New Phytologist* **218**, 885–890 (2018).
- 614 Dimichele, W. A., Pfefferkorn, H. W. & Gastaldo, R. A. RESPONSE OF LATE  
615 CARBONIFEROUS AND EARLY PERMIAN PLANT COMMUNITIES TO CLIMATE  
616 CHANGE 1. (2001).

- 616 Falcon-Lang, H. J. & Bashforth, A. R. Morphology, anatomy, and upland ecology of large  
618 cordaitalean trees from the Middle Pennsylvanian of. *Rev Palaeobot Palynol* **135** (3–4), 223–  
619 243 (2005).
- 620 Falcon-Lang, H. J. & Bashforth, A. R. Pennsylvania uplands were forested by giant  
621 cordaitalean trees. *Geology* **32**, 417–420 (2004).
- 622 Bashforth, A. R. (Arden R., Canadian Society of Petroleum Geologists. & Geological  
623 Association of Canada. Late Carboniferous (Bolsovian) macroflora from the Barachois  
624 Group, Bay St. George Basin, southwestern Newfoundland, Canada. 123 (2005).
- 625 Davies, N. S. & Gibling, M. R. The sedimentary record of Carboniferous rivers: Continuing  
626 influence of land plant evolution on alluvial processes and Palaeozoic ecosystems. *Earth Sci*  
627 *Rev* **120**, 40–79 (2013).
- 628 Alexander, J., Fielding, C. R. & Jenkins, G. Plant-material deposition in the tropical Burdekin  
629 River, Australia: implications for ancient fluvial sediments. *Palaeogeogr Palaeoclimatol*  
630 *Palaeoecol* **153**, 105–125 (1999).
- 631 Melrose, C. S. A. Fossilized Forests of the Lower Carboniferous Horton Bluff Formation,  
632 Nova Scotia. (2003).
- 633 Wagner, R. H. & Diez, J. B. Verdeña (Spain): Life and death of a Carboniferous forest  
634 community. *C R Palevol* **6**, 495–504 (2007).
- 635 Stewart, W. N. (Wilson N. & Rothwell, G. W. Paleobotany and the evolution of plants. 521  
636 (2009).
- 637 Phillips, T. L. & Dimichele, W. A. Comparative Ecology and Life-History Biology of  
638 Arborescent Lycopods in Late Carboniferous Swamps of Euramerica. *Annals of the Missouri*  
639 *Botanical Garden* **79**, 560–588 (1992).
- 640 Hagerty, D. J., Spoor, M. F. & Ullrich, C. R. Bank failure and erosion on the Ohio river. *Eng*  
641 *Geol* **17**, 141–158 (1981).
- 642 Thorne, C. R., Russell, A. P. G. & Alam, M. K. Planform pattern and channel evolution of  
643 the Brahmaputra River, Bangladesh. *Geological Society, London, Special Publications* **75**,  
644 257–276 (1993).
- 645 Coleman, J. M. Brahmaputra river: Channel processes and sedimentation. *Sediment Geol* **3**,  
646 129–239 (1969).
- 647 Martin, C. A. L. & Turner, B. R. Origins of massive-type sandstones in braided river systems.  
648 *Earth Science Reviews* **44**, 15–38 (1998).
- 649 Robison, E. G. & Beschta, R. L. Characteristics of coarse woody debris for several coastal  
650 streams of southeast Alaska, USA. *Canadian Journal of Fisheries and Aquatic Sciences* **47**,  
651 1684–1693 (1990).
- 652 Fielding, C. R. Upper flow regime sheets, lenses and scour fills: Extending the range of  
653 architectural elements for fluvial sediment bodies. *Sediment Geol* **190**, 227–240 (2006).
- 654 Hansford, M. R., Plink-Björklund, P. & Jones, E. R. Global quantitative analyses of river  
655 discharge variability and hydrograph shape with respect to climate types. *Earth Sci Rev* **200**,  
656 102977 (2020).
- 657 Cotter, E. Paleoflow characteristics of a late Cretaceous river in Utah from analysis of  
658 sedimentary structures in the Ferron Sandstone. *J Sediment Petrol* **41**, 129–142 (1971).
- 659 Miall, A. D. Reconstructing fluvial macroform architecture from two-dimensional outcrops:  
660 examples from the Castlegate Sandstone, Book Cliffs, Utah. *Journal of Sedimentary*  
661 *Research* **B64**, 146–158 (1994).
- 662 Hampson, G. J., Jewell, T. O., Irfan, N., Gani, M. R. & Bracken, B. Modest change in fluvial  
663 style with varying accommodation in regressive alluvial-to-coastal-plain wedge: Upper  
664 Cretaceous Blackhawk Formation, Wasatch Plateau, central Utah, U.S.A. *Journal of*  
665 *Sedimentary Research* **83**, 145–169 (2013).

- 666 Flood, Y. S. & Hampson, G. J. Facies and architectural analysis to interpret avulsion style  
667 and variability: Upper Cretaceous Blackhawk Formation, Wasatch Plateau, Central Utah,  
668 U.S.A. *Journal of Sedimentary Research* **84**, 743–762 (2014).
- 669 Serinaldi, F., Loecker, F., Kilsby, C. G. & Bast, H. Flood propagation and duration in large  
670 river basins: a data-driven analysis for reinsurance purposes. *Natural Hazards* **94**, 71–92  
671 (2018).
- 672 Gastaldo, R. A. & Huc, A.-Y. Sediment facies, depositional environments, and distribution of  
673 phytoclasts in the recent Mahakam River Delta, Kalimantan, Indonesia. *Palaios* **7**, (1992).
- 674 Hayden, A. T., Lamb, M. P. & McElroy, B. J. Constraining the Timespan of Fluvial Activity  
675 From the Intermittency of Sediment Transport on Earth and Mars. *Geophys Res Lett* **48**,  
676 (2021).
- 677 Martin, R. L. & Jerolmack, D. J. Origin of hysteresis in bed form response to unsteady flows.  
678 *Water Resour Res* **49**, 1314–1333 (2013).
- 679 Mahon, R. C. & McElroy, B. Indirect estimation of bedload flux from modern sand-bed  
680 rivers and ancient fluvial strata. *Geology* **46**, 579–582 (2018).
- 681 Gupta, P. K., Chauhan, S. & Oza, M. P. Modelling surface run-off and trends analysis over  
682 India. *J. Earth Syst. Sci.* **125**, 1089–1102 (2016).
- 683 Waters, C. N., Waters, R. A., Barclay, W. J. & Davies, J. R. *A lithostratigraphical framework*  
684 *for the Carboniferous successions of southern Great Britain (onshore)*. (2009).
- 685 Barclay, W. J. *Geology of the Swansea District - A brief explanation of the geological map.*  
686 *Shet explanation of the British Geological Survey. 1:50,000 Sheet 247 Swansea (England and*  
687 *Wales)*. (2011).

688

## 689 ACKNOWLEDGEMENTS

690 The authors acknowledge research support from Imperial College London. We are grateful to  
691 Gary Hampson and Cedric John for useful feedback on an early version of the manuscript.

## 692 AUTHOR CONTRIBUTIONS

693 **JSM:** Data curation (lead), formal analysis (lead), investigation (lead), methodology (lead),  
694 visualization (lead), visualisation (lead), writing – original draft (lead), writing – review and  
695 editing (equal); **JW:** Data curation (supporting), formal analysis (supporting), investigation  
696 (supporting), methodology (supporting), writing – review and editing (equal); **SJL:** Data  
697 curation (supporting), formal analysis (supporting), investigation (supporting), methodology  
698 (supporting), supervision (supporting), writing – review and editing (equal); **JV:** Formal  
699 analysis (supporting) investigation (supporting), methodology (supporting), writing – review  
700 and editing (supporting); **ARTS:** Formal analysis (supporting), investigation (supporting),  
701 writing – review and editing (supporting); **ACW:** Principal investigation, Data curation  
702 (supporting), formal analysis (supporting), methodology (supporting), supervision (lead),  
703 writing – review and editing (equal).

704 **COMPETING INTERESTS**

705 The authors declare no competing interests.

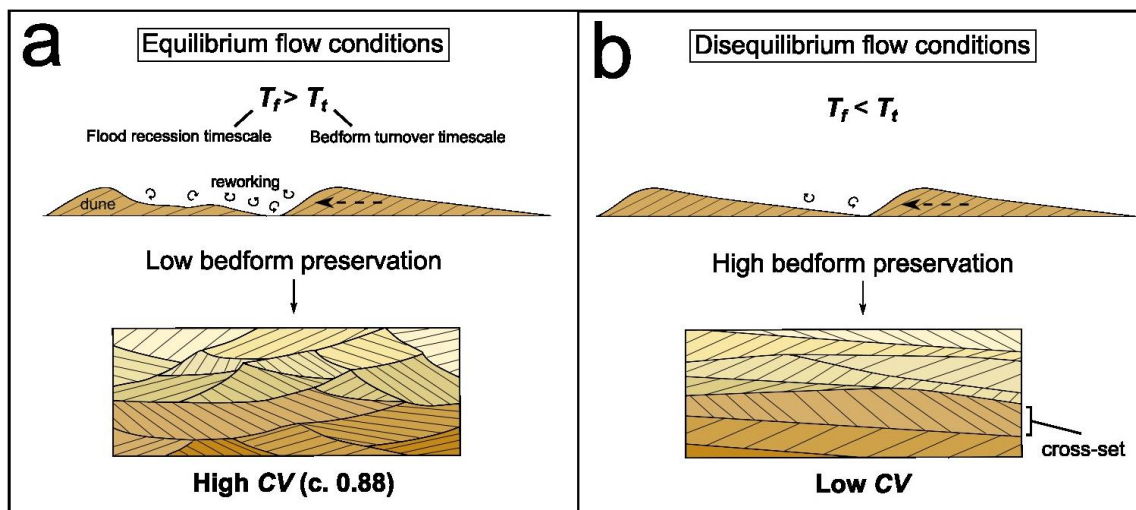
706 **Tables**

Parameter	Definition	References
<b>Mean cross set height, <math>h_{xs}</math></b>	The mean from a distribution of heights measured within one cross-set.	21,22
<b>Original bedform height, <math>h_d</math></b>	The original height of the bedform before preservation as a cross-set. $h_d = 2.9(\pm 0.7)h_{xs}$	
<b>Bedform preservation ratio, <math>h_{xs}/h_d</math></b>	The ratio of cross-set height to original bedform height, representing the proportion of the original height of the bedform preserved in the rock record.	13,20
<b>Coefficient of variation of cross-set height, <math>CV</math></b>	The ratio of standard deviation to mean of cross-set height, measured along a single cross-set. $CV = \frac{\sigma}{\mu}$ $\sigma$ : standard deviation $\mu$ : mean	21,22
<b>Bedform turnover timescale, <math>T_t</math></b>	The length of time taken for a bedform to be fully reworked by flow, or for the sediment in a dune to be displaced downstream by one bedform wavelength. $T_t = \frac{\lambda h_d \beta}{q_b}$ $\lambda$ : dune wavelength ( $\approx 7.3H$ ) $\beta$ : shape factor ( $\approx 0.55$ ) $q_b$ : unit bedload flux	12,13,70
<b>Prevailing flow duration, <math>T_f</math></b>	The duration of the falling limb of the discharge event which generated the preserved bedform. $T_f = T_t T^*$ $T^*$ : bedform disequilibrium number	12,13
<b>Flow intermittency factor, <math>I_f</math></b>	The fraction of the total time in which bankfull flow would accomplish the same amount of water discharge as the real hydrograph. $I_f = \frac{\Sigma Q(t)}{Q_{bf} \Sigma t}$ $\Sigma Q(t)$ : sum of the time dependent discharge $Q_{bf}$ : bankfull discharge $\Sigma t$ : timespan	68

707 Table 1: Key palaeohydrological variables and definitions.

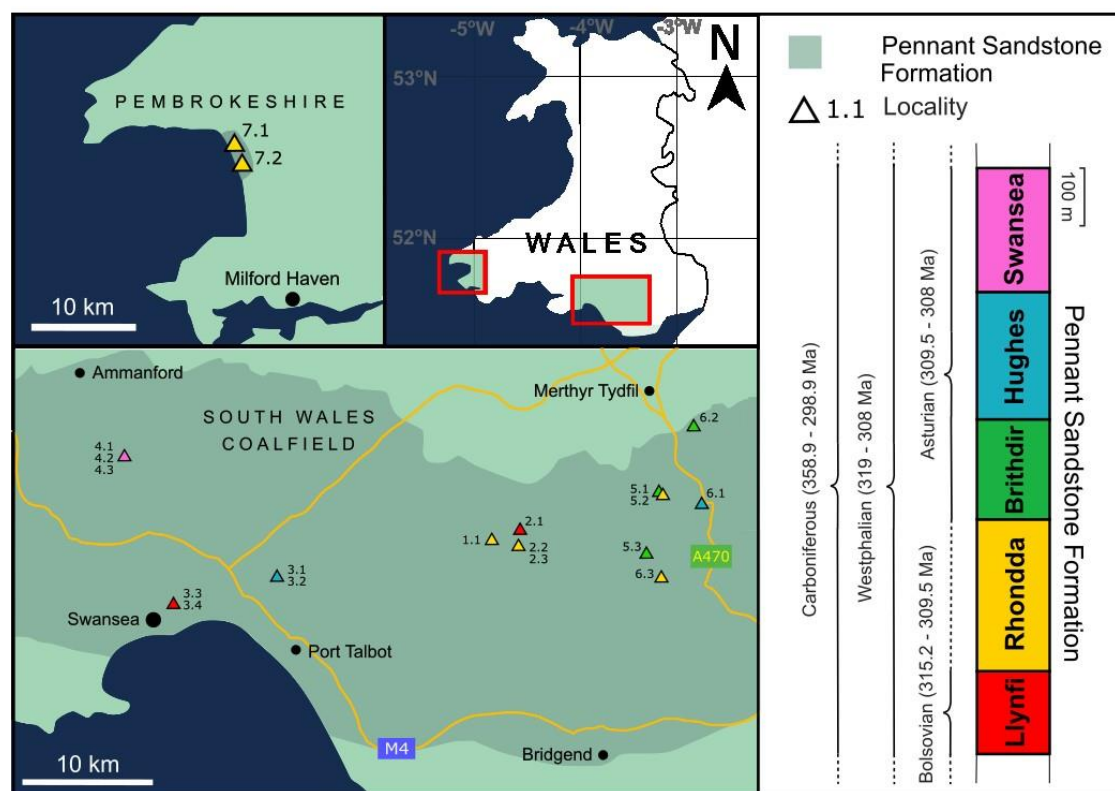
708 **Figure Captions**

709



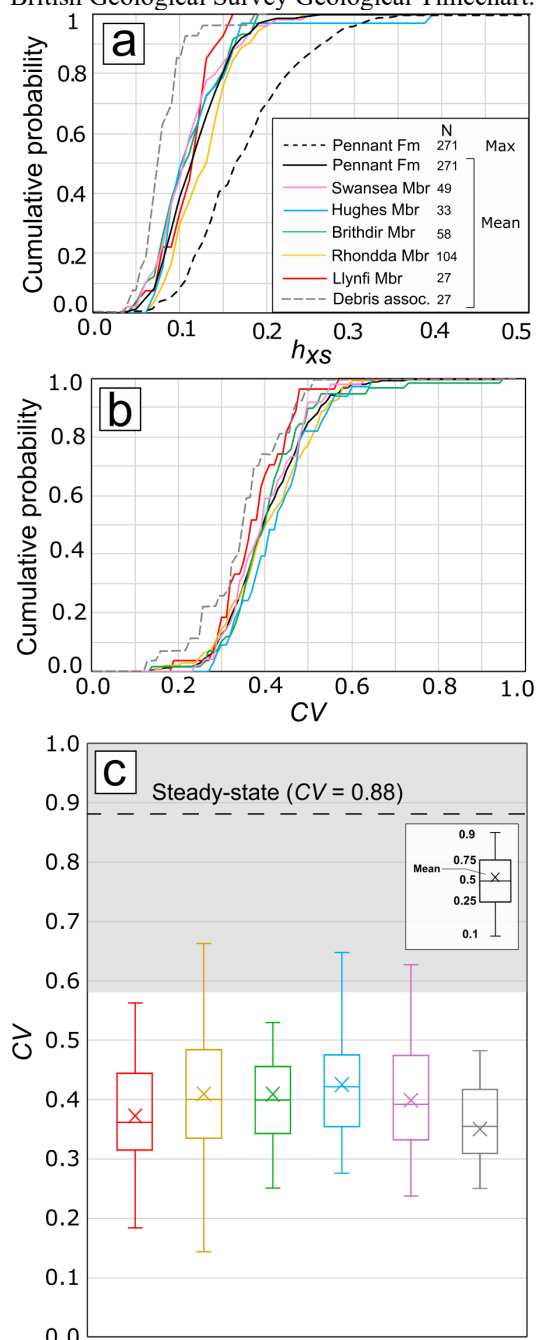
710

711 Figure 1: The hydrodynamic conditions that lead to differences in coefficient of variation of cross-set  
 712 height,  $CV$ , recorded in cross-strata. (a) Dune migration and evolution in steady-state (equilibrium) flow  
 713 conditions, and the resultant geometries of preserved cross-sets; (b) dune evolution and preservation in  
 714 disequilibrium with prevailing flow, resulting in low  $CV$ .



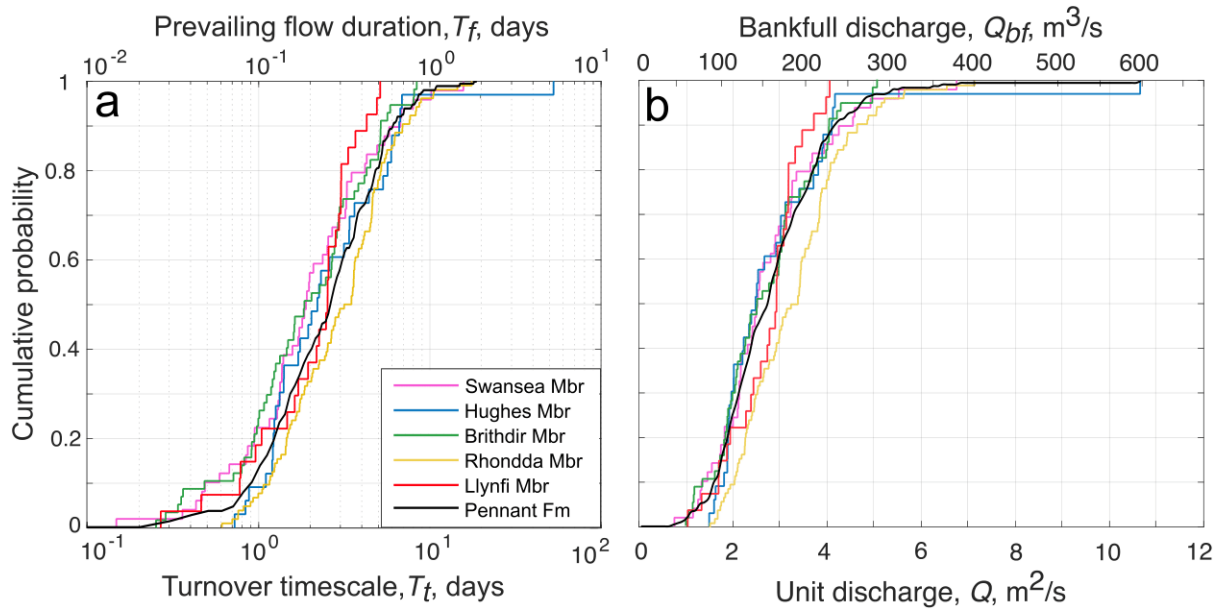
715

716 Figure 2: The South Wales and Pembrokeshire Coalfields, and the localities used for primary data  
 717 collection. Pennant Formation geology is outlined after Jones and Hartley<sup>35</sup>. The stratigraphic column shows the  
 718 five Members of the Pennant Formation, modified from Waters et al<sup>72</sup>, and Barclay<sup>73</sup> with age data from the



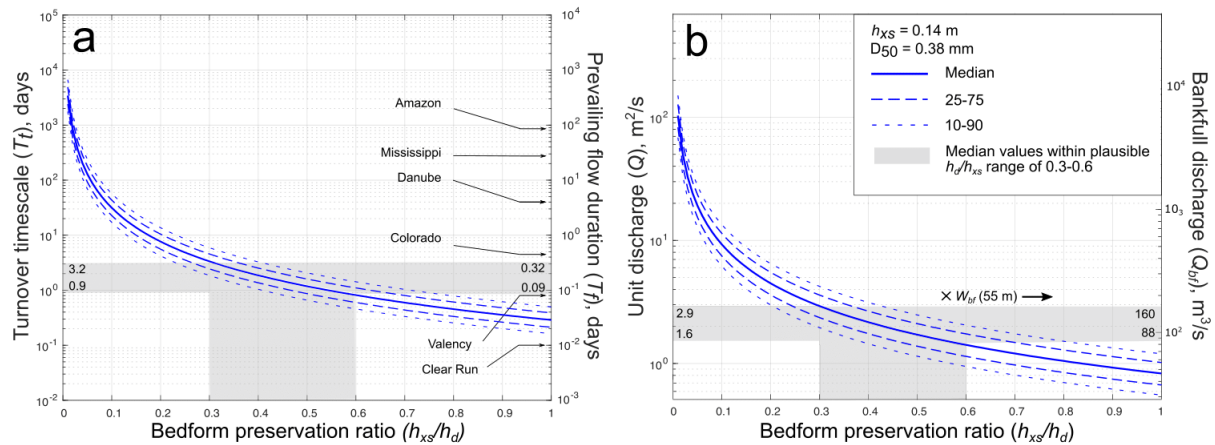
721 **Figure 3: Cross-set data demonstrating disequilibrium bedform preservation.** (a) Cumulative probability  
 722 distributions of mean cross-set height for each member of the Pennant Formation, with distributions of the  
 723 mean, 84<sup>th</sup> percentile, maximum for the Pennant Formation overall, and cross-sets associated with woody  
 724 debris; (b) similar to (a), but with distributions of CV; (c) the CV of cross-set height for each member of the  
 725 Pennant Formation. The dashed line and grey shaded region indicate the theoretical and empirical range of CV  
 726 at steady state of  $0.88 \pm 0.3^{21,22}$ , and the grey box represents cross-sets associated with woody debris.





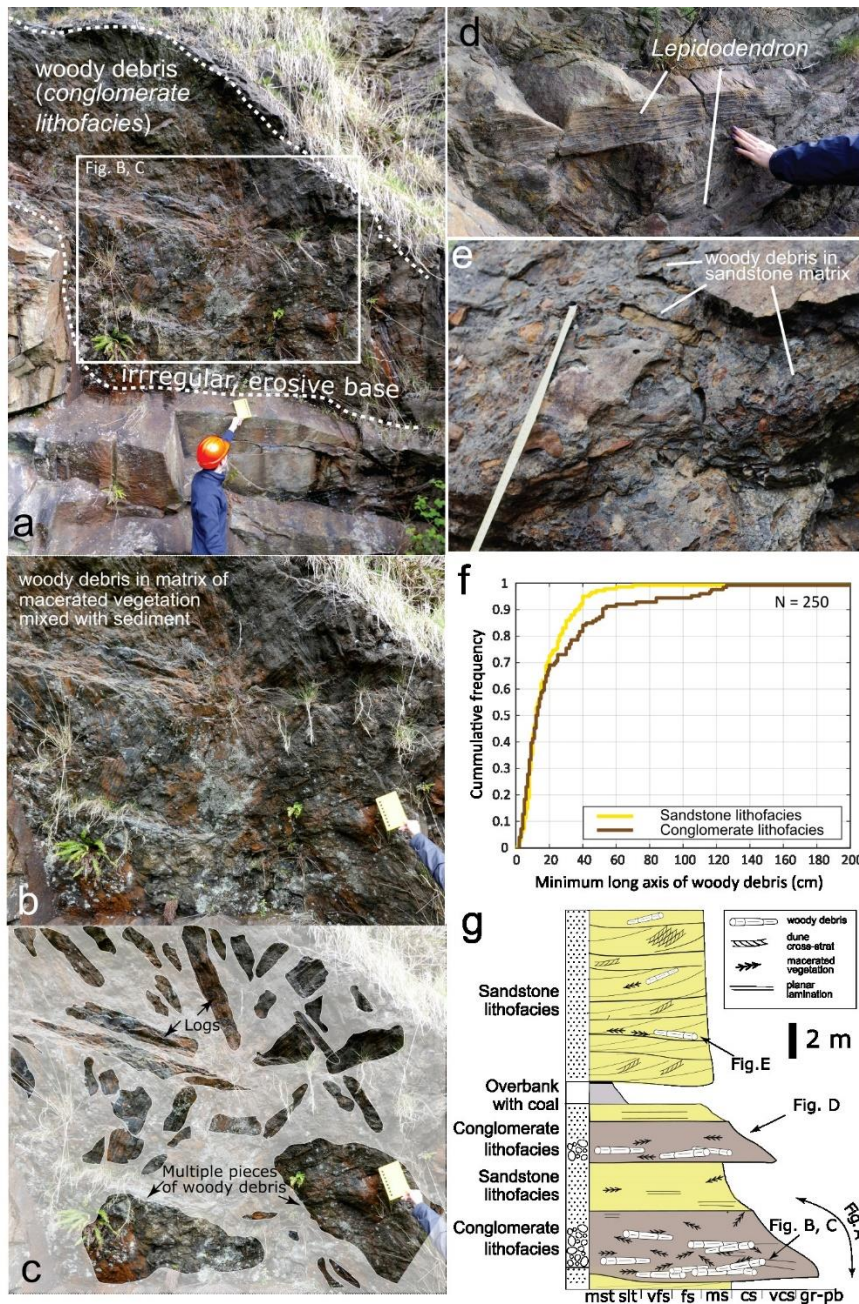
727

728 Figure 4: **Cumulative probability distribution graphs showing key palaeohydrological variables.** (a) The  
 729 primary x-axis represents bedform turnover timescale,  $T_t$ , in each member of the Pennant Formation, and the  
 730 secondary x-axis indicates prevailing flow duration,  $T_f$ , which we set as  $0.1T_t$ , following Leary and Ganti<sup>13</sup>; (b)  
 731 the primary x-axis represents the unit discharge,  $Q$ , and the secondary x-axis represents the bankfull discharge,  
 732  $Q_{bf}$ , calculated by multiplying  $Q$  by the average width of the channel,  $55 \text{ m}^{28}$ .



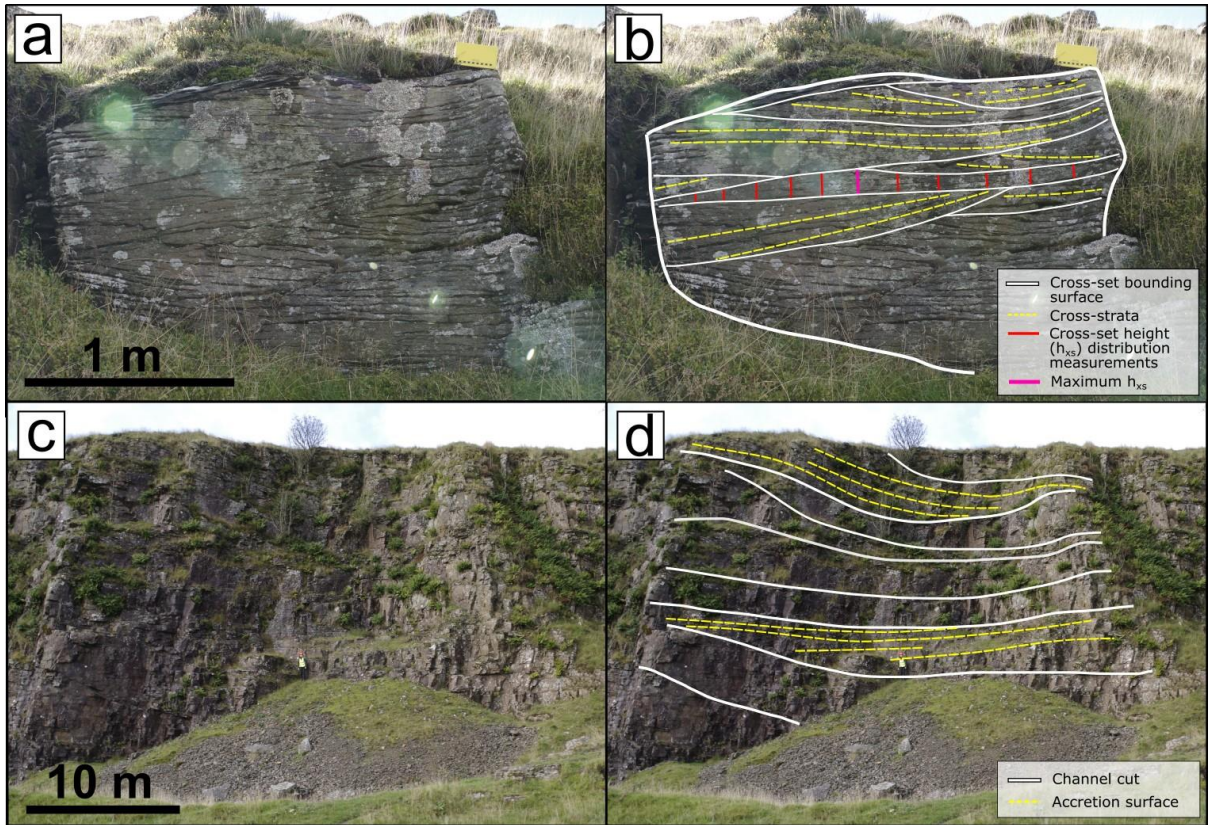
733

734 Figure 5: **The effect of increased bedform preservation ratios on key palaeohydrological parameters.** (a) The  
 735 primary y-axis indicates bedform turnover timescale,  $T_t$ , and the secondary y-axis indicates prevailing flow  
 736 duration,  $T_f$ , when bedform disequilibrium number,  $T^*$ , is set as  $0.1^{13}$ , and  $T_f$  of 6 modern rivers are given for  
 737 comparison (references in Supplementary Material); (b) the primary y-axis indicates unit discharge,  $Q$ , and the  
 738 secondary y-axis indicates bankfull discharge,  $Q_{bf}$ , when channel width is set as  $55 \text{ m}$ , the average for the  
 739 Pennant Formation<sup>28</sup>.



740

741 **Figure 6: Examples of woody debris in the Pennant Formation, specifically in the Llynfi Member, at**  
 742 **Kilvey Hill, Loc3.3.** (a) The underside of the erosional base of a log-jam deposit in the *conglomerate*  
 743 *lithofacies*, in which clasts comprise plant debris as opposed to rock fragments, overlying channel sandstone; (b,  
 744 c) a closer view of this outcrop, with the largest woody debris fossils highlighted, noting that the matrix is  
 745 composed of a mixture of sediment and macerated vegetation; (d) an example of well-preserved *Lepidodendron*  
 746 fossils; (e) a debris bed in the *sandstone lithofacies*; (f) the cumulative frequency distribution of the minimum  
 747 long axis of debris fossil found in the *sandstone* and *conglomerate lithofacies*; and (g) a schematic log  
 748 displaying the typical features of the *conglomerate* and *sandstone lithofacies* in the Pennant Formation, using  
 749 Kilvey Hill as an exemplar.



750

751 Figure 7: **Field measurements at outcrop.** (a, b) Methods of collecting cross-set height measurements, where  
 752 the vertical bars make one cross-set height distribution, Locality 6.2; (c, d) architectural elements observed at  
 753 outcrop scale, including accretion surfaces for use in Equation 7, Locality 2.1.

754